iMRI

Investigative
Magnetic
Resonance
Imaging

The Imaging Features of Desmoid Tumors: the Usefulness of Diffusion Weighted Imaging to Differentiate between Desmoid and Malignant Soft Tissue Tumors

Seung Baek Lee, Soon Nam Oh, Moon Hyung Choi, Sung Eun Rha, Seung Eun Jung, Jae Young Byun

Department of Radiology, Seoul St. Mary's Hospital, College of Medicine, The Catholic University of Korea, Seoul, Korea

Original Article

Purpose: To evaluate the imaging findings of desmoid tumors using various imaging modalities and to evaluate whether diffusion-weighted imaging (DWI) can help differentiate between desmoid and malignant tumors.

Materials and Methods: The study included 27 patients with pathologically confirmed desmoid tumors. Two radiologists reviewed 23 computed tomography (CT), 12 magnetic resonance imaging (MRI) and 8 positron emission tomography-computed tomography (PET-CT) scans of desmoid tumors and recorded data regarding the shape, multiplicity, size, location, degree of enhancement, and presence or absence of calcification or hemorrhage. The signal intensity of masses on T1- and T2-weighted imaging and the presence or absence of whirling or band-like low signal intensity on T2-weighted imaging were recorded. The apparent diffusion coefficient (ADC) values of the desmoid tumors in nine patients with DWIs were compared with the ADC values of 32 malignant tumors. The maximum standardized uptake value (SUV_{max}) on PET-CT images was measured in 8 patients who underwent a PET-CT.

Results: The mean size of the 27 tumors was 6.77 cm (range, 2.5-26 cm) and four tumors exhibited multiplicity. The desmoid tumors were classified by shape as either mass forming (n = 18), infiltrative (n = 4), or combined (n = 5). The location of the tumors was either intra-abdominal (n = 15), within the abdominal wall (n = 8) or extra-abdominal (n = 4). Among the 27 tumors, 21 showed moderate to marked enhancement and 22 showed homogeneous enhancement. Two tumors showed calcifications and one displayed hemorrhage. Eleven of the 12 MR T2-weighted images showed whirling or band-like low signal intensity areas in the mass. The mean ADC value of the desmoid tumors (1493×10^{-6} mm^2/s) was significantly higher than the mean of the malignant soft tissue tumors (873×10^{-6} mm^2/s, P < 0.001). On the PET-CT images, all tumors exhibited an intermediate SUV_{max} (mean, 3.7; range, 2.3-4.5).

Conclusion: Desmoids tumors showed homogenous, moderate to marked enhancement on CT and MRI scans and a characteristic whirling or band-like pattern on T2-weighted images. DWI can be useful for the differentiation of desmoid tumors from malignant soft tissue tumors.

Keywords: CT; MRI; Desmoid Tumor; Fibromatosis; DWI

iMRI

INTRODUCTION

Desmoid tumors, also known as aggressive fibromatosis, are rare and comprise only 0.03% of all neoplasms and 3% of all soft-tissue tumors. They usually occur sporadically, but approximately 5% of cases are associated with familial adenomatous polyposis (FAP) that occurs in Gardner syndrome (1-4). Desmoid tumors are benign fibromatous tumors characterized by histopathologically abnormal fibroblastic/myofibroblastic proliferation and marked accumulation of intracellular collagen (5-7). They can arise from any part of the body and are classified into the intra-abdominal, abdominal wall, and extra-abdominal subtypes according to location (8, 9). Although histologically benign, desmoid tumors are often locally invasive and associated with a high local recurrence rate after resection (3, 10). They are generally asymptomatic; however, various symptoms occur as a result of the compressive or obstructive effects on other organs (2, 3, 11).

Previously reported findings of the imaging of desmoid tumors demonstrated varying degrees of homogeneous enhancement on CT and MRI scans and may show a mass-forming or infiltrative growth pattern (2, 9, 11). However, the imaging findings of desmoid tumors reported thus far are very diverse and often similar to those of malignant tumors in signal intensity (SI), tumor margination, and in the tendency to encase adjacent organs (12-14). Therefore, the diagnosis of desmoid tumors is a challenge for both radiologists and clinicians. A diffusion-weighted image (DWI) is widely used for a variety of tumors or disease entities. Several previous studies have reported that DWI can distinguish malignant tumors from benign tumors (15); however, there was only one report regarding the DWI of primarily desmoid tumors in the extremities. In this study, we compared the imaging features and DWI findings of desmoid tumors that were primarily located in the abdomen of patients with intra-abdominal malignant tumors. We also tried to compare the PET-CT findings between desmoid tumors and intra-abdominal malignancies. The purpose of this study was to evaluate the imaging findings of desmoid tumors, using various imaging modalities including CT, MRI and PET-CT, and to evaluate whether DWI can help differentiate desmoid tumors from other intra-abdominal or abdominal wall malignancies.

METHODS AND MATERIALS

Patients

This study received a study-specific Institutional Review Board approval and waiver of informed consent. A total of 27 patients who were diagnosed with a pathologically confirmed desmoid tumor between 2005 and 2016 were enrolled in the study. Twenty-six patients were diagnosed with desmoids tumors by surgical resection and one patient by needle biopsy.

Four patients had a family history of FAP; 4 patients had a history of colorectal cancer; and, 13 patients had a history of surgery. Of 27 patients, 23 underwent CT, 12 underwent MRI including 9 with a DWI, and 8 patients underwent PET-CT before surgery.

Thirty-two patients, who were pathologically confirmed as having a malignant soft tissue tumor from 2009 to 2015, were also enrolled in order to compare their apparent diffusion coefficient (ADC) values with those of the desmoid tumors. The malignant soft tissue tumors included liposarcomas (n = 4), malignant peripheral nerve sheath tumors (n = 4), gastrointestinal stromal tumors (n = 4), endometrial stromal sarcomas (n = 3), rhabdomyosarcomas (n = 2), leiomyosarcomas (n = 2), lymphomas (n = 2), squamous cell carcinomas (n = 2), Ewing sarcoma (n = 1), malignant melanoma (n = 1), primitive neuroendocrine tumor (n = 1), dermatofibrosarcoma protuberans (n = 1), malignant solitary fibrous tumor (n = 1), synovial sarcoma (n = 1), myeloid sarcoma (n = 1), carcinosarcoma (n = 1), and malignant spindle cell tumor (n = 1).

Computed Tomography

All CT scans were performed using one of the following commercially available multi-detector CT scanners: Sensation 64 (Siemens Medical Solutions, Erlangen, Germany); LightSpeed VCT (GE Medical Systems, Milwaukee, WI, USA): or Volume Zoom (Siemens Medical Solutions, Erlangen, Germany). Every patient received 100-150 mL of an intravenous contrast agent (iopromide, Ultravist 300; Bayer Schering Healthcare, Berlin, Germany) at a rate of 3 mL/s. The scanning parameters were as follows: slice thickness, 0.625-1 mm; beam pitch, 1/1; gantry rotation time, 0.5/0.5 sec; and tube voltage, 100-120 kV(p). The data were reformatted in the axial and coronal planes with a 5-mm section thickness at 5-mm intervals. Readers reviewed all CT images with a picture archiving and communication system workstation (Marotech 5.4, Seoul, Korea).

iMRI

CT and MRI Features of Desmoid Tumors | Seung Baek Lee, et al.

Magnetic Resonance Imaging

Three patients underwent MRI using a 1.5-T MRI scanner (Magnetom Vision Plus; Siemens) and 9 patients underwent MRI using a 3-T MR scanner (Magnetom Verio; Siemens Medical Solutions, Erlangen, Germany) with a phased-array coil. MRI was performed with the following sequences: 1) a sagittal T2-weighted fast spin-echo sequence; 2) an axial T1-weighted fast spin-echo sequence (TR/TE 750/10; flip angle 120~150; field of view [FOV] 200 × 200-350 × 350 mm; matrix size 320 × 224; 2-4 NEX; slice thickness 5 mm with no gap); and, 3) an axial T2-weighted fast spin echo sequence (TR/TE 4000/118; flip angle 120-140; FOV 200 × 200-350 × 350 mm; matrix size 320 × 224; 2 NEX; slice thickness 5 mm with no gap). Diffusion-weighted MR images were performed in the axial plane using a single shot-echo planar imaging technique with a b factors of 0, 500, and 1000 sec/mm^2, TR/TE 6100-9000/83, FOV 200-350 mm, matrix size 120 × 80, 2 NEX, and a slice thickness of 5 mm with no slice gap. The contrast-enhanced T1-weighted image with fat suppression on the axial plane with TR/TE 640/13, flip angle 150, and a slice thickness of 5 mm was obtained after an intravenous injection of 0.1 mmol/kg Gadobutrol (Gadovist, Schering, Berlin, Germany) or gadopentetate dimeglumine (Magnevist; Schering, Berlin, Germany) at a rate of 3 mL/s followed by a 30-mL saline flush.

Positron Emission Tomography – Computed Tomography

Each patient fasted for 6 hours before the PET/CT examination. Scanning started one hour after an intravenous injection of ^{18}F-FDG (370-555 MBq) from the orbitomeatal line to the upper thigh. No intravenous contrast agent was administered. Studies were obtained via combined PET/CT in-line systems, specifically either the Biograph Duo or Biograph TruePoint (Siemens Medical Solutions, Knoxville, TN, USA). Six to eight bed positions were used and the acquisition time was 2 minutes per bed position. The CT scanned from the orbitomeatal line to the proximal thigh (120 kV, 50 mAs, and 5-mm slice thickness; 130 kV) and PET was performed over the same body region. The CT data were used for attenuation correction and image reconstruction was performed with a standard ordered-subset expectation maximization algorithm (OSEM; two iterations, eight subsets). The axial spatial resolution was approximately 6.5-4.5 mm. All PET/CT images were reviewed with fusion software (Syngo; Siemens Medical Solutions, Knoxville, TN, USA) that provided multiplanar reformatted images and displayed PET images with attenuation correction, CT images, and PET/CT fusion images.

Image Interpretation – Qualitative Analysis

Two radiologists with 15 and 3 years of experience, respectively, reviewed 23 CT and 12 MR images of desmoid tumors in consensus and recorded data regarding the shape, multiplicity, size, location, degree of enhancement, presence or absence of calcification or hemorrhage and pattern of T2-weighted imaging on MRI. The shape of the mass was classified into mass-forming, infiltrative, and combined forms. The location of the mass was classified into abdominal wall, intra-abdominal and extra-abdominal groups. The degree of enhancement was classified as mild, moderate, or marked relative to the adjacent muscle's enhancement, and homogeneity of enhancement was visually assessed as homogeneous or heterogeneous by two radiologists in consensus on the CT or/and MR images. For the 12 patients who underwent MRI, the signal intensities of the masses on the T1- and T2-weighted imaging were classified as low, intermediate, and high as compared to the adjacent muscle's signal intensity. Whirling or band-like patterns were defined as elongated or stripe-like repeated low signal intensity lesions on the T2-weighted MRI (Fig. 1), and the presence or absence of whirling or band-like patterns was recorded for each mass. Furthermore, we compared the imaging features of the MRI scans between
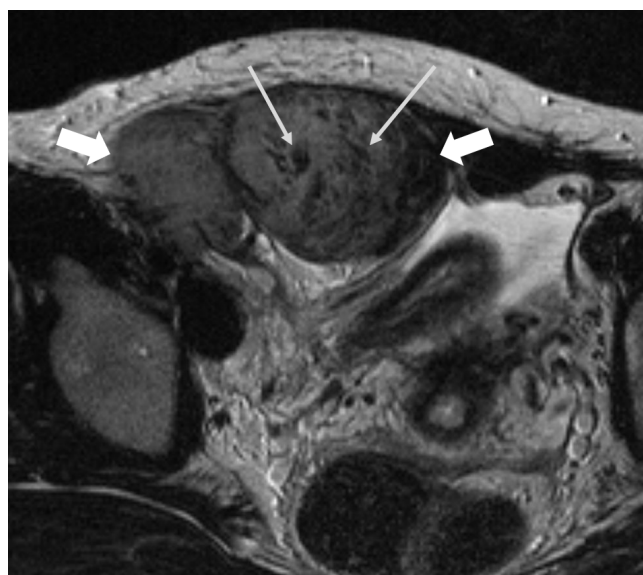

Fig. 1. MR T2-weighted image of a 34-year-old female patient with an abdominal wall desmoid tumor (white arrows) shows internal whirling or band-like low signal intensities (long white arrows).

the desmoid tumors and 32 malignant soft tissue tumors arising from the abdominal cavity or wall, including the signal intensities on T1- and T2-weighted imaging, enhancement degree, homogeneity, and the presence or absence of dark SI whirling or bank-like patterns on the T2-weighted image.

Image Interpretation – Quantitative Analysis

Nine patients underwent diffusion-weighted images. In eight patients, three regions of interest (ROIs) of approximately 1.0 cm × 1.0 cm were manually placed on the ADC map and ADC values were recorded by averaging the values for the three ROIs (Fig. 2a, b). Only one ROI was obtained for one patient who had a small lesion (maximum diameter was 2.0 cm).

In addition, we enrolled 32 patients with pathologically confirmed malignant soft tissue tumors arising from the abdominal cavity or wall in order to compare the ADC
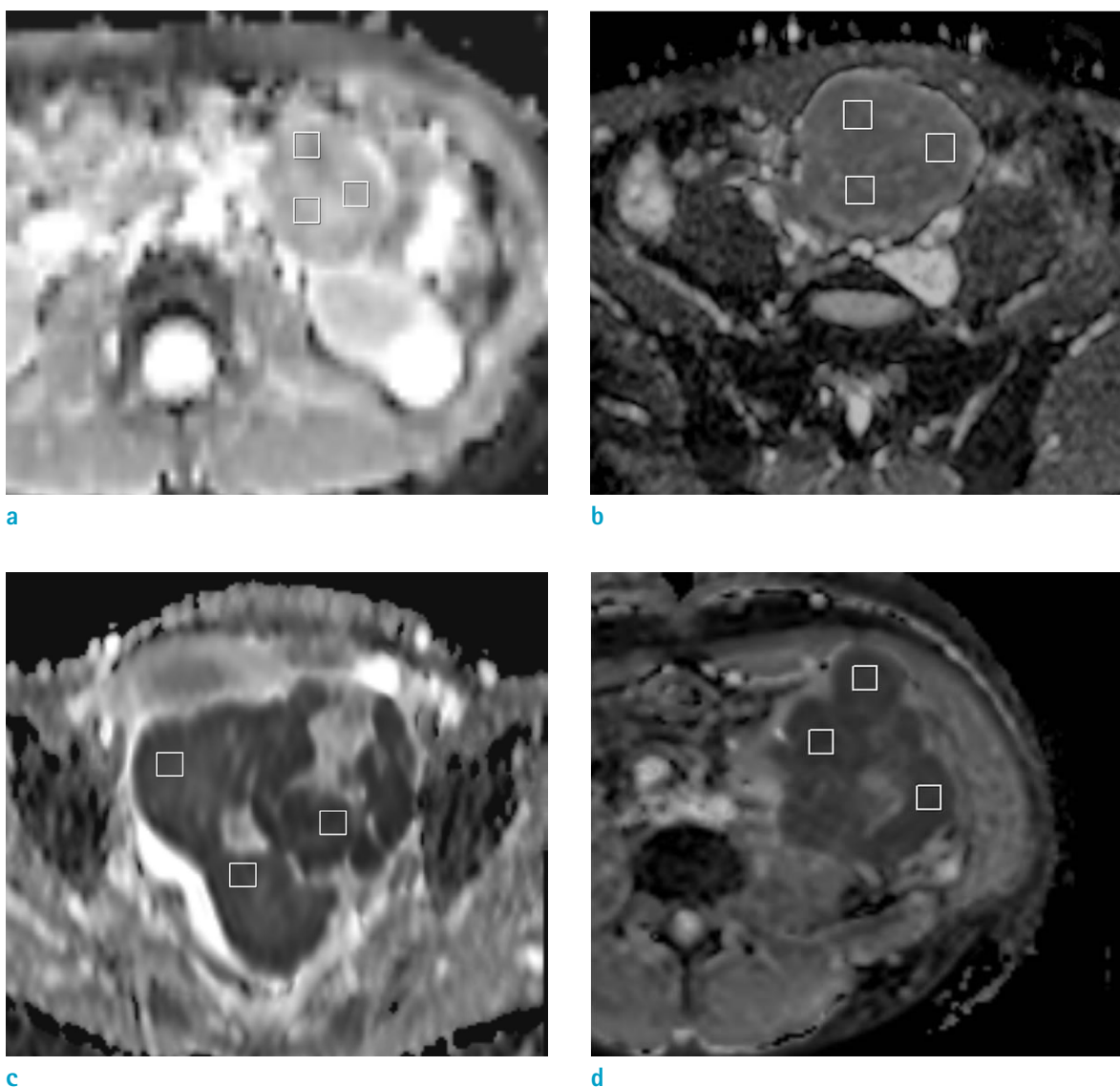

a

b

c

d

Fig. 2. ADC maps of desmoid tumors (a, b), and malignant soft tissue tumors (c, d). (a) Intra-abdominal desmoid tumor in a 31-year-old male patient and (b) intra-abdominal desmoid tumor in a 32-year-old male patient. (c) Intra-abdominal malignant soft tissue tumor (primitive neuroectodermal tumor) in a 32-year-old female patient and (d) intra-abdominal malignant soft tissue tumor (retroperitoneal malignant solitary fibrous tumor) in a 69-year-old male patient. Three white squares (approximately 1.0 cm × 1.0 cm) in each ADC map represent the regions of interest within the tumors.

iMRI

CT and MRI Features of Desmoid Tumors | Seung Baek Lee, et al.

values between the desmoid tumors and malignant soft tissue tumors. Three ROIs were manually placed on the ADC map and the ADC values of the 3 ROIs were measured as above for each malignant tumor (Fig. 2c, d).

The maximum standardized uptake values (SUV_{max}) of the eight desmoid tumors and thirty-two malignant soft tissue tumors on the PET/CT images were measured with the Syngo fusion software. This step applied to the eight patients who had underwent a PET-CT.

A Mann-Whitney U test was used to determine whether the differences between the ADC values and SUV_{max} of the desmoid and malignant soft tissue tumors were statistically significant.

RESULTS

Table 1 summarizes the clinical data for the 27 patients who had desmoid tumors (age range, 20-80 years; mean age, 46 years; male:female = 11:16). The mean tumor size was 6.77 cm (range, 2.5-26 cm; standard deviation [SD], 5.21 cm). Intra-abdominal (n = 15), abdominal wall (n = 8) and extra-abdominal (n = 4) tumors were present.

The tumors were related to FAP in four patients. The remaining patients had sporadic desmoid tumors. Thirteen patients had a positive history for operations including colectomy, Cesarean section, and cholecystectomy. The qualitative imaging characteristics of the tumors are presented in Table 1. The most common tumor shape was mass forming (n = 18), followed by infiltrative (n = 4) and combined (n = 5). Most tumors were solitary, though four showed multiplicity (4/27). Most of the desmoid tumors showed moderate or marked enhancement (21/27) and homogeneous enhancement (22/27). The presence of calcification (n = 2) and hemorrhage (n = 1) were unusual findings in the desmoid tumors.

MR characteristics are presented in Table 2. Most of the desmoid tumors showed low to intermediate signal intensity on the T1-weighted images and intermediate to high signal intensity on the T2-weighted images. The whirling or band-like pattern was seen in 11 of the 12 desmoid tumors. The 32 malignant soft tissue tumors showed low to intermediate signal intensities on the T1-weighted image (24/32) and intermediate to high signal intensities on the T2-weighted image (14 high, 16 intermediate). Four of the 32 malignant tumors showed a whirling or band-like pattern on the T2-weighted image. The malignant tumors typically displayed moderate to marked contrast enhancements (26 marked,

3 moderate, 3 mild) with a heterogeneous enhancement (21/32). All desmoid tumors and malignant soft tissue

Table 1. Clinical and Qualitative Imaging Features of 27 Patients with a Desmoid Tumor

Characteristic, n = 27	Number or mean (range) (%)
Sex	
Female	16 (59.3)
Male	11 (40.7)
Age (mean, range)	46 (20-80)
Image modalities	
CT only	9 (33.4)
CT + PET-CT	7 (25.9)
CT + MRI	6 (22.2)
MRI only	4 (14.8)
CT + MRI + PET-CT	1 (3.7)
Location	
Intraabdominal	15 (55.6)
Abdominal wall	8 (29.6)
Extraabdominal	4 (14.8)
FAP (+)	4 (14.8)
Colon cancer history (+)	4 (14.8)
Operation history (+)	13 (48.1)
Multiplicity	
Solitary	23 (85.2)
Multiple	4 (14.8)
Size (cm)	6.77 (2.5-26)
Shape	
Mass forming	18 (66.7)
Infiltrative	4 (14.8)
Combined	5 (18.5)
Enhancement degree	
Marked	9 (33.4)
Moderate	12 (44.4)
Mild	6 (22.2)
Homogeneity	
Homogeneous	22 (81.5)
Heterogeneous	5 (18.5)
SUV_{max} on PET-CT	3.7 (2.3-4.5)

(+) = presence; CT = computed tomography; FAP = familial adenomatous polyposis; MRI = magnetic resonance imaging; PET-CT = positron emission tomography-computed tomography; SUV_{max} = maximum standardized uptake value

iMRI

Table 2. MR Imaging Characteristics of Desmoid Tumors

Patient No.	SI on T1WI	SI on T2WI	Low SI whirling on T2WI	Presence of DWI	Mean ADC value
15	Low	Intermediate	+	−	
16	Low	Intermediate	+	−	
17	Low	High	+	+	1645
18	Low	Low	+	+	1654
19	Low	Intermediate	+	+	1309
20	Low	High	+	−	
21	Low	Intermediate	+	+	1476
22	Low	High	+	+	1697
23	Low	Intermediate	+	+	1268
24	Intermediate	Intermediate	+	+	1204
25	Intermediate	Intermediate	−	+	1354
26	Intermediate	Intermediate	+	+	1828

+ = presence; − = absence; ADC = apparent diffusion coefficient; DWI = diffusion-weighted image; SI = signal intensities; T1WI = T1-weighted image; T2WI = T2-weighted image

Unit of mean ADC value: 10^{-6} mm^2/s

tumors exhibited high signal intensities on the DWI scans. The mean ADC value of the desmoid tumors was 1493 × 10^{-6} (min: 1204 × 10^{-6} mm^2/s, max: 1828 × 10^{-6} mm^2/s, SD: 221 × 10^{-6} mm^2/s), which was significantly higher than that of the malignant soft tissue tumors (mean: 873 × 10^{-6} mm^2/s, min: 370 × 10^{-6} mm^2/s, max: 1503 × 10^{-6} mm^2/s, SD: 273 × 10^{-6} mm^2/s, P < 0.001; Fig. 3).

On the PET-CT images, the mean SUV_{max} of the desmoid tumors (mean, 3.7; 2.3-4.5 ± 0.72; Fig. 4) was significantly lower than that of the malignant soft tissue tumors (mean, 10.9; 3.3-33.7 ± 7.39, P < 0.001).

DISCUSSION

Fibromatosis is a rare mesenchymal tumor characterized histologically by the proliferation of fibroblasts and myofibroblasts with the production of intracellular collagen (2, 5). Fibromatosis can be classified according to its anatomical location into superficial and deep fibromatosis, which show different genetic backgrounds and clinical behavior (9, 16, 17). Superficial fibromatosis arises from fascia or aponeuroses in the extremities including palmar, plantar, penile and knuckle pad locations and usually exhibits less symptomatic and slow-growing features compared to deep fibromatosis. Deep fibromatosis usually originates from the connective tissue in the muscles, fascia, or aponeurosis, and can be further classified into three
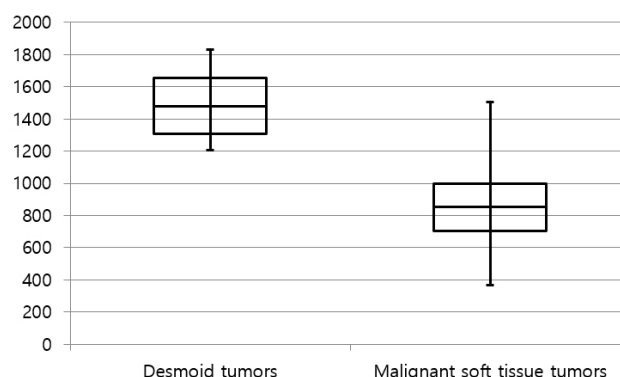

Fig. 3. Box plot distribution of the mean ADC values of the desmoid and malignant soft tissue tumors. Box = 25th-75th percentile; horizontal line = median. The mean ADC value of desmoid tumors (mean: 1493 × 10^{-6} mm^2/s, min: 1204 × 10^{-6} mm^2/s, max: 1828 × 10^{-6} mm^2/s, SD: 221 × 10^{-6} mm^2/s) was significantly higher than that of the malignant soft tissue tumors (mean: 873 × 10^{-6} mm^2/s, min: 370 × 10^{-6} mm^2/s, max: 1503 × 10^{-6} mm^2/s, SD: 273 × 10^{-6} mm^2/s; P < 0.001). The Y-axis represents apparent diffusion coefficient (ADC) values. Unit of ADC value: 10^{-6} mm^2/s.

subgroups: intra-abdominal, abdominal wall or extra-abdominal location. Deep fibromatosis is often known to be more aggressive and related to genetic differences. The imaging findings and symptoms of deep fibromatosis varied according to the location of the mass (5). In our study, all cases are classified as deep fibromatosis and the
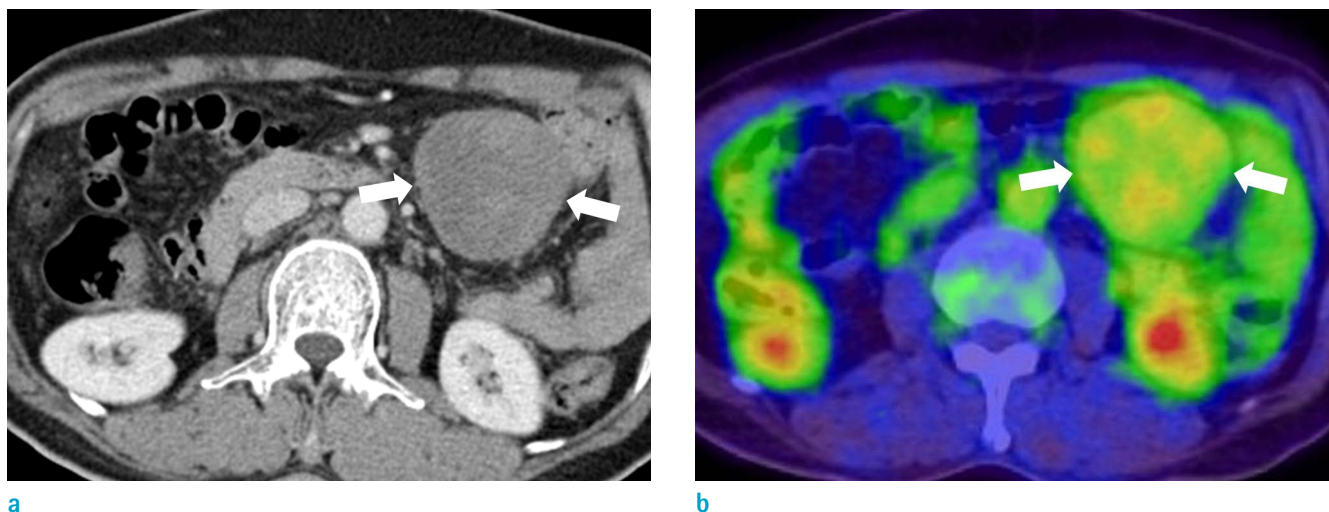
167

iMRI

CT and MRI Features of Desmoid Tumors | Seung Baek Lee, et al.

a

b

Fig. 4. A 64-year-old male patient with an intra-abdominal desmoid tumor. The contrast enhanced CT axial image (a) shows homogeneous enhancing soft tissue mass (arrow) in the peritoneal cavity. The PET-CT image (b) shows moderate increased uptake of the mass (arrows) (SUV_{max}=2.3).

majority of cases (85%, n=23/27) were located at the intra-abdominal or abdominal wall. Because of the aggressive growth pattern of deep fibromatoses, the differentiation of intra-abdominal malignant soft tissue tumor is usually challenging.

In our study, most desmoid tumors showed a mass forming or infiltrative shape with moderate or marked homogeneous enhancement and rarely seen calcification or necrosis in the masses. These findings were similar and consistent with previous reports (10, 11, 18). Recently, several MRI features of desmoid tumors have been reported and some researchers have correlated the various signal intensities of the mass on the T2-weighted images with histopathologic findings such as cellular, collagen, and myxoid components through the excellent soft tissue contrast resolution of MRI (6, 14, 19). Consistent with previous reports (20), most of the desmoid tumors in our study also showed T2 low signal intensity band-like lesions (so called band sign) that corresponded with pathologically dense collagenous stroma. Because this finding is characteristic but not necessarily specific to desmoid tumors, the same may be seen in other benign and malignant soft tissue tumors (20). Some malignant tumors in our cases also showed T2 low signal intensity band or nodular areas less frequently (12.5%, n = 4/32) than the desmoid tumors did (91.7%, n = 11/12). In addition to the frequency, the morphological characteristics of a low signal intensity band in the malignant tumors were somewhat different to those of the desmoid tumors. The

T2 low signal intensity band seen in the desmoid tumors were regular and small; whereas, those seen in malignant tumors appeared irregular and ugly. Further studies with a radiologic-pathologic correlation will be needed for a pathologic explanation of T2 low SI in malignant tumors.

It is still challenging for radiologists to distinguish desmoid tumors from malignant masses solely by qualitative imaging characteristics. The recent widespread use of DWI has allowed quantitative assessment of water diffusion in the tissue, which is expressed by the ADC. Several previous studies have reported that DWI can distinguish malignant tumors from benign tumors in a variety of locations (15, 21); however, few studies have reported the features of the desmoid tumors on DWI. Oka et al. (15) compared ADC values of 8 desmoid tumors with those of 74 malignant tumors. They found a significant difference in the ADC values between the desmoid and malignant soft tissue tumors. In their report, the mean ADC value of the desmoid tumors was $1.36 \pm 0.48 \times 10^{-3}$ mm^2/s (mean $\pm$ SD), which is similar to the ADC value of the desmoid tumors of our study ($1.47 \pm 0.80 \times 10^{-3}$ mm^2/s). The higher ADC value of the desmoid tumors compared with malignant tumors may be due to low cellularity caused by the marked production of intercellular collagen in the desmoid tumors (15, 22). Oka et al. (15) reported the usefulness of DWI for differentiating between desmoid and malignant soft tissue tumors, but most of the masses were extra-abdominal and mainly located at the extremity; therefore, only 3 abdominal

tumors were included. Extra-abdominal desmoid tumors displayed a somewhat different growth pattern than found in the abdominal wall or intra-abdominal desmoid tumors (8, 16). In our series, among the 9 patients with DWI, 7 lesions were located in the abdominal cavity or abdominal wall. Therefore, we compared the desmoid tumors with malignant tumors arising from the abdominal cavity or abdominal wall and found a significant difference in ADC values. This result may be useful for distinguishing desmoid tumors from malignant tumors that are specifically arising from the intra-abdominal cavity or abdominal wall. In particular, intra-abdominal or abdominal wall desmoid tumors found during the postoperative follow-up examination of abdominal malignancies are difficult to differentiate from the recurrence or seeding metastasis of malignancy. We believe that DWI would be a useful diagnostic tool in these cases.

The imaging findings of desmoid tumors on PET-CT, which is usually performed for the evaluation of malignancy, are not well known. In a previous study (9), the maximum standardized uptake values (SUV_{max}) of the desmoid tumors ranged from 3.4 to 5.4, which is similar to the values found in our study (mean 3.7, 2.4-4.5). Our study demonstrated that the mean SUV_{max} of the desmoid tumors was significantly lower than that of the malignant tumors. Thus, the SUV_{max} value of the PET-CT scans might also be useful for the differentiation of desmoid tumors from malignancy.

Our study has some limitations. First, the number of patients with a desmoid tumor was small and imaging modalities used for tumor assessment were not uniform, but included CT, MRI and PET-CT. This is because desmoid tumors are very rare and the duration of patient collection for our study was long (12 years). Future investigations need to include a larger sample size and a standard imaging modality. Second, we could not correlate the MR image findings of the desmoid tumors with their pathologic findings on a case-by-case basis.

In conclusion, desmoid tumors usually displayed relatively homogeneous enhancement on the CT and MRI scans and a characteristic whirling or band-like pattern on T2-weighted imaging. The desmoid tumors also showed higher ADC values on DWI and intermediate SUV_{max} values on PET-CT compared with malignant soft tissue tumors. Because the findings of the qualitative assessment on the CT and MRI scans may overlap with those of malignant tumors, the quantitative assessment including DWI can be useful for the diagnosis of desmoid tumors and differentiation them from malignant tumors.

REFERENCES

1. Azizi L, Balu M, Belkacem A, Lewin M, Tubiana JM, Arrive L. MRI features of mesenteric desmoid tumors in familial adenomatous polyposis. AJR Am J Roentgenol 2005;184:1128-1135
2. Shinagare AB, Ramaiya NH, Jagannathan JP, et al. A to Z of desmoid tumors. AJR Am J Roentgenol 2011;197:W1008-1014
3. de Bree E, Keus R, Melissas J, Tsiftsis D, van Coevorden F. Desmoid tumors: need for an individualized approach. Expert Rev Anticancer Ther 2009;9:525-535
4. Healy JC, Reznek RH, Clark SK, Phillips RK, Armstrong P. MR appearances of desmoid tumors in familial adenomatous polyposis. AJR Am J Roentgenol 1997;169:465-472
5. Dinauer PA, Brixey CJ, Moncur JT, Fanburg-Smith JC, Murphey MD. Pathologic and MR imaging features of benign fibrous soft-tissue tumors in adults. Radiographics 2007;27:173-187
6. Lee JC, Thomas JM, Phillips S, Fisher C, Moskovic E. Aggressive fibromatosis: MRI features with pathologic correlation. AJR Am J Roentgenol 2006;186:247-254
7. Liu P, Thorner P. MRI of fibromatosis: with pathologic correlation. Pediatr Radiol 1992;22:587-589
8. Casillas J, Sais GJ, Greve JL, Iparraguirre MC, Morillo G. Imaging of intra- and extraabdominal desmoid tumors. Radiographics 1991;11:959-968
9. Walker EA, Petscavage JM, Brian PL, Logie CI, Montini KM, Murphey MD. Imaging features of superficial and deep fibromatoses in the adult population. Sarcoma 2012;2012:215810
10. Hayashi K, Takamura M, Yokoyama H, et al. A mesenteric desmoid tumor with rapid progression. Intern Med 2017;56:505-508
11. Shields CJ, Winter DC, Kirwan WO, Redmond HP. Desmoid tumours. Eur J Surg Oncol 2001;27:701-706
12. Kransdorf MJ, Jelinek JS, Moser RP Jr, et al. Magnetic resonance appearance of fibromatosis. A report of 14 cases and review of the literature. Skeletal Radiol 1990;19:495-499
13. Sheth PJ, Del Moral S, Wilky BA, et al. Desmoid fibromatosis: MRI features of response to systemic therapy. Skeletal Radiol 2016;45:1365-1373
14. Vandevenne JE, De Schepper AM, De Beuckeleer L, et al. New concepts in understanding evolution of desmoid tumors: MR imaging of 30 lesions. Eur Radiol 1997;7:1013-1019
15. Oka K, Yakushiji T, Sato H, et al. Usefulness of diffusion-weighted imaging for differentiating between desmoid tumors and malignant soft tissue tumors. J Magn Reson Imaging 2011;33:189-193

iMRI

CT and MRI Features of Desmoid Tumors | Seung Baek Lee, et al.

16. Hartman TE, Berquist TH, Fetsch JF. MR imaging of extraabdominal desmoids: differentiation from other neoplasms. AJR Am J Roentgenol 1992;158:581-585
17. Xu H, Koo HJ, Lim S, et al. Desmoid-type fibromatosis of the thorax: CT, MRI, and FDG PET characteristics in a large series from a tertiary referral center. Medicine (Baltimore) 2015;94:e1547
18. Einstein DM, Tagliabue JR, Desai RK. Abdominal desmoids: CT findings in 25 patients. AJR Am J Roentgenol 1991;157:275-279
19. Sundaram M, McGuire MH, Schajowicz F. Soft-tissue masses: histologic basis for decreased signal (short T2) on T2-weighted MR images. AJR Am J Roentgenol

1987;148:1247-1250
20. Braschi-Amirfarzan M, Keraliya AR, Krajewski KM, et al. Role of imaging in management of desmoid-type fibromatosis: a primer for radiologists. Radiographics 2016;36:767-782
21. Le Bihan D, Breton E, Lallemand D, Grenier P, Cabanis E, Laval-Jeantet M. MR imaging of intravoxel incoherent motions: application to diffusion and perfusion in neurologic disorders. Radiology 1986;161:401-407
22. Manenti G, Di Roma M, Mancino S, et al. Malignant renal neoplasms: correlation between ADC values and cellularity in diffusion weighted magnetic resonance imaging at 3 T. Radiol Med 2008;113:199-213